

Thermal Conductivity of Molten Lead-Free Solders¹

J. Bilek,² J. K. Atkinson,² and W. A. Wakeham^{2,3}

The paper reports measurements of the thermal conductivity of a number of molten solders for the electronics industry that are part of a group of materials designed to be free of the toxic problems associated with lead-based solders. The measurements have been carried out with a transient hot-wire instrument originally designed for the measurement of the thermal conductivity of pure molten metals. In the application reported here the instrument has been used largely unchanged but an improved finite-element code has been used for the analysis of the raw data so as to yield the thermal conductivity of the molten solders. The measurements extend from the melting point of the solder up to 625 K. The uncertainty in the thermal conductivity measurements is estimated to be no larger than 3%.

KEY WORDS: lead free; molten solders; thermal conductivity; transient hot-wire technique.

1. INTRODUCTION

The production of modern electronic circuitry requires the careful design of soldering processes and involves operation on a very small scale with considerable precision using valuable components. For that reason there is increasing attention being devoted to the modeling of the soldering process during manufacture and, in particular, to the heat transfer processes that inevitably accompany it. The thermal conductivity of the molten solder is an especially significant parameter to those models. At the same

¹ Paper presented at the Seventh Asian Thermophysical Properties Conference, August 23–28, 2004, Hefei and Huangshan, Anhui, P. R. China.

² School of Engineering Sciences, University of Southampton, Southampton SO17 1BJ, United Kingdom.

³ To whom correspondence should be addressed. E-mail: vice-chancellor@soton.ac.uk

time there is a strong movement to exclude from modern solder materials components that are hazardous to health such as lead [1]. The latter fact means that there is a strong desire to introduce into industrial production a number of new solders that are devoid of lead. However, the thermal properties of these new materials, particularly the thermal conductivity, are unknown. For that reason we have implemented a program of measurement to study the thermal conductivity of these new materials over a range of temperature from their melting point up to 625 K. In the current work we study two new lead-free solders for the electronics industry and compare the values obtained with those for standard lead-based solders. The measurements have been carried out with an instrument developed over the last decade [2] that is applied to mixtures of molten metals for the first time.

2. EXPERIMENTAL

The transient hot-wire instrument [3] has become one of the instruments of choice for the measurement of the thermal conductivity of simple, often organic, liquids under temperatures not far removed from ambient. It has the unique advantage among macroscopic techniques that transient measurements in a temperature gradient generated by a heating process are made so quickly that there can be no substantive contribution of convective heat flow in the system. Realization of a similar benefit for measurements in fluids that are electrically conducting and potentially chemically aggressive has proved more difficult. Initial attempts for electrically conducting liquids near ambient conditions employed techniques in which the transient hot wire was anodized to introduce an electrically insulating layer [3]. While this proved successful at temperatures that departed but modestly from ambient, further measures were needed to extend the technique to the much higher temperatures needed to study many molten metals.

A first step in the development of the transient hot-wire technique for application to molten metals was reported by Peralta-Martinez, Wakeham and their collaborators [2, 4]. In their application the metallic hot wire of platinum is sandwiched between two thin rectangular substrates of alumina which permit connections to the wire for measurement purposes. It is this instrument that is employed for the measurements reported here and the sensor, which forms its heart, is shown in Fig. 1. The platinum wire (25 μm diameter) is attached to a system of electrodes of platinum thick film printed on one side of a green alumina substrate with a thickness of 300 μm . The conducting lines are arranged so that the wire itself has two parts, a shorter section and a longer section, each of which can have its

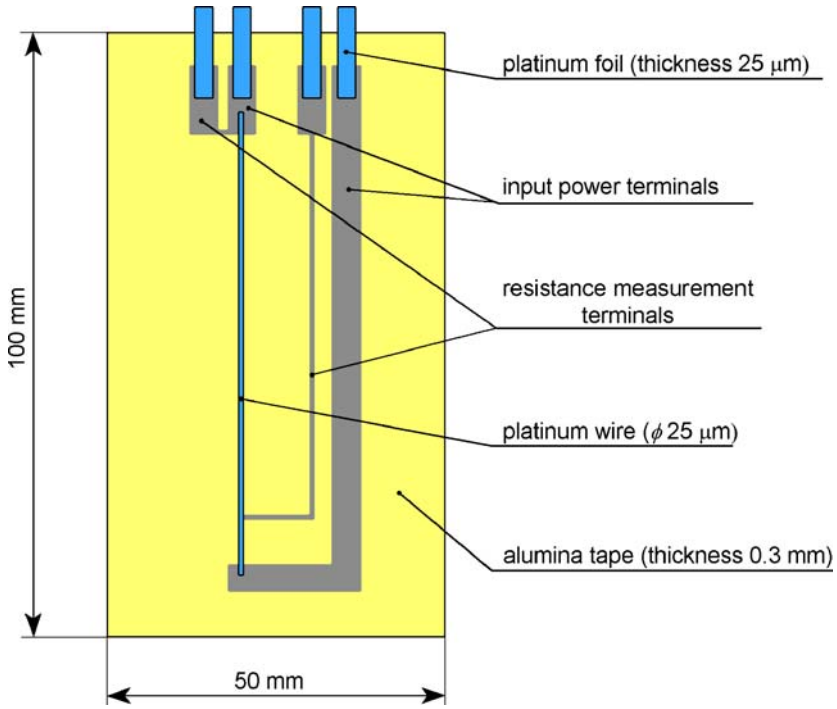


Fig. 1. Plan view of the thermal conductivity sensor.

resistance measured independently in a four-terminal manner by an appropriate bridge. This assembly is covered with a second sheet of identical alumina which is bonded to the first by heating under pressure, and the entire assembly is then baked to fire the alumina in an oven and carefully constrained to produce uniform shrinkage of the alumina sheets in their own plane but no distortion perpendicular to the plane.

The basic concept of the experiments with this sensor remains that of the transient hot-wire method [3]. An electrical current is initiated in the wire at time $t=0$, and the dissipation causes the temperature of the wire to rise in a manner determined by the thermal properties of the materials surrounding the wire. Unlike the simple hot-wire case, here the fluid surrounds the sensor which contains the circular wire imbedded in an alumina substrate. Thus, the evolution of the temperature of the wire following the initiation of the heat pulse involves the properties of the alumina and its shape as well as the properties of the wire and the fluid. Thus, while it is still possible to determine the temperature rise of the wire from transient measurements of its resistance, the relationship of that measurement to the thermal

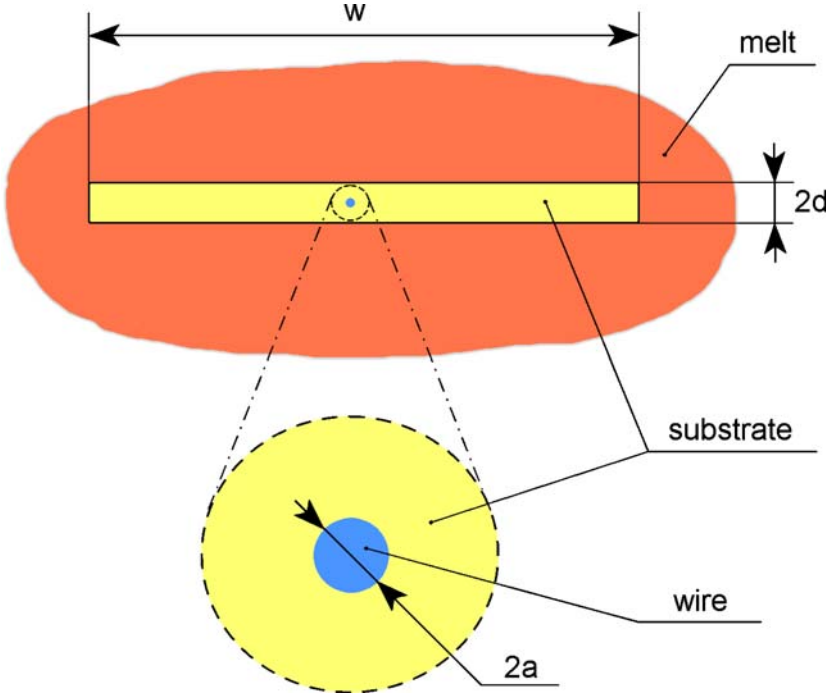


Fig. 2. Cross section of the sensor as the basis of a mathematical model.

conductivity of the fluid is considerably more complex than for the standard hot-wire system. For that reason, the theoretical description of the current experiment is achieved by way of a numerical solution of the appropriate heat transfer equations rather than with a simple analytical equation. Figure 2 contains a cross-sectional view of the sensor and defines its geometry for use in the formulation of the equations of heat transfer. Since the measurement system is arranged so as to cancel any non-uniformities in temperature in the z -direction, it is possible to treat the problem as one in two dimensions [4].

In fact, the relevant equations governing the evolution of the temperature, T , of the wire at time t after application of a heat flux q per unit length in the wire are [2, 4, 5] for the wire:

$$\rho_w C_{Pw} \frac{\partial T_w}{\partial t} = \lambda_w \left[\frac{\partial^2 T_w}{\partial x^2} + \frac{\partial^2 T_w}{\partial y^2} \right] + \frac{q}{\pi a^2} \tag{1}$$

for the substrate material:

$$\rho_s C_{Ps} \frac{\partial T_s}{\partial t} = \lambda_s \left[\frac{\partial^2 T_s}{\partial x^2} + \frac{\partial^2 T_s}{\partial y^2} \right] \quad (2)$$

for the melt:

$$\rho_m C_{Pm} \frac{\partial T_m}{\partial t} = \lambda_m \left[\frac{\partial^2 T_m}{\partial x^2} + \frac{\partial^2 T_m}{\partial y^2} \right] \quad (3)$$

where a is the radius of the platinum wire and the symbols ρ, λ, T , and C_P represent the density, thermal conductivity, temperature, and heat capacity, respectively. The subscripts w, s , and m indicate wire, substrate, and melt, respectively. The solution of these equations is subject to the following initial and boundary conditions:

1. Initial condition for $t = 0$

$$T_w = T_s = T_m = T_0 \quad \text{for all } x, y \quad (4)$$

2. Boundary conditions for $t > 0$

For the wire-substrate interface, along $x^2 + y^2 = a^2$

$$T_w = T_s \quad (5)$$

and

$$\lambda_w \frac{\partial T_w}{\partial r} = \lambda_s \frac{\partial T_s}{\partial r} \quad (6)$$

For the substrate-melt interface

when $y = -d, x = 0$ to $\pm w/2$

and $y = d, x = 0$ to $\pm w/2$

$$T_m = T_s \quad (7)$$

$$\lambda_m \frac{\partial T_m}{\partial x} = \lambda_s \frac{\partial T_s}{\partial x} \quad (8)$$

$$\lambda_m \frac{\partial T_m}{\partial y} = \lambda_s \frac{\partial T_s}{\partial y} \quad (9)$$

while for $x \rightarrow \infty$ or $y \rightarrow \infty$

$$T_m = T_0 \quad t > 0 \quad (10)$$

This system of equations can be solved using a finite-element method to an accuracy better than or equal to that achieved in an experimental measurement. The grid system employed for the present work is shown in Fig. 3. It is an enhancement over that employed in earlier work [2, 4] since it is no longer necessary to approximate the shape of the circular wire by means of an appropriately chosen square [2].

In other respects the experimental procedure and the details of the equipment remain as before [2]. The sensor is suspended in an alumina cup containing the molten metal within a vertical, tubular furnace shown in Fig. 4 at temperatures varying from several degrees above the melting point of the solder to approximately 625 K.

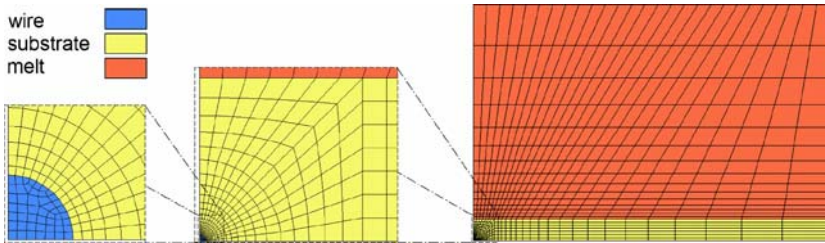


Fig. 3. Mesh employed for 2D finite-element model of the cross section of the sensor and melt.

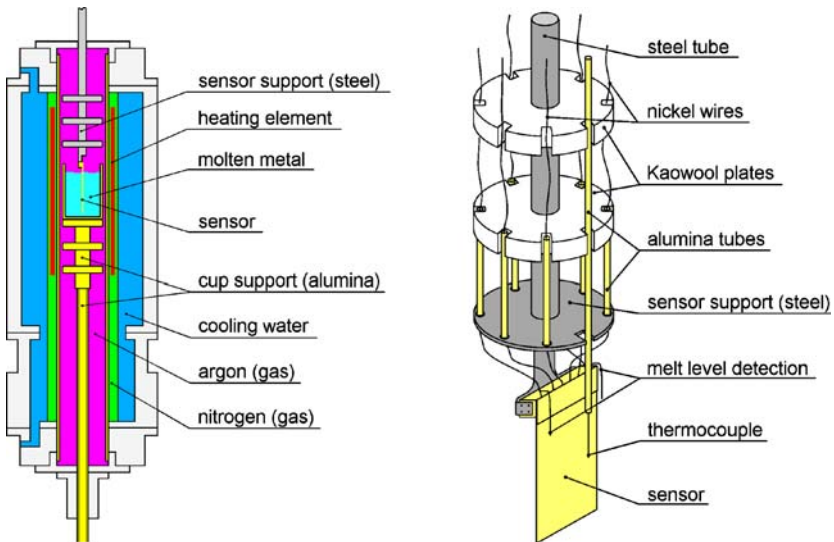


Fig. 4. Tubular furnace housing the molten-metal crucible and the sensor with details on the sensor support configuration.

The heating current applied to the hot wire is generated by two power supplies which are remotely controlled. They are supplying a bridge which is arranged to measure the out-of-balance signal generated by the differential resistance change of the short and long parts of the platinum hot wire. Voltage values are measured at several thousand points during the transient increase of temperature of about 5–7 K over a period of about a second [2]. This system automatically compensates for the effects at the ends of the hot wire, and thus the bridge yields the resistance change arising from a finite section of wire without ends. In turn, this resistance measurement is converted into a temperature rise using the resistance-temperature characteristics of platinum.

In order to derive the thermal conductivity of the molten material around the sensor from the measured temperature rise, the finite-element model solution of the working equations is carried out with iterative estimates of the thermal conductivity and specific heat capacity of both the substrate and the melt. Values for the thermal properties of platinum are taken from the literature [6].

The samples of solder were supplied by MBO (UK), Ltd. We have studied one alloy of tin and lead which is in common commercial use, one with 60% tin (Sn60Pb40) and a second leaded solder containing 62% tin, 36% lead, and 2% silver. Among unleaded solders, we have studied alloys of tin with copper (Sn99.3Cu0.7) and tin with silver and copper (Sn95.5Ag3.8Cu0.7).

3. RESULTS

As with all measurements, it is important to verify that the theoretical model of the experiment is consistent with what is observed in practice. Figure 5 contains a plot of the deviations of the measured temperature rise for an experimental run in the lead/tin sample. The temperature rise of the wire during this run was about 7 K so that the observed deviations amount to at most 0.15% of the temperature rise which is consistent with the precision of the temperature rise measurements. This degree of agreement confirms that the apparatus operates in accord with the theory. The structure of the deviation plot reveals small effects resulting from the interfaces between the various media which indicate that the boundary conditions of the interfaces assumed in the theory are not exactly obeyed. Also, it can be seen that the deviations tend to show a periodic behavior especially after 0.01 s from the start of the experiment. This phenomenon arises from inaccuracies which are caused by time-stepping in the transient FE model employed in this work. More recently [7]

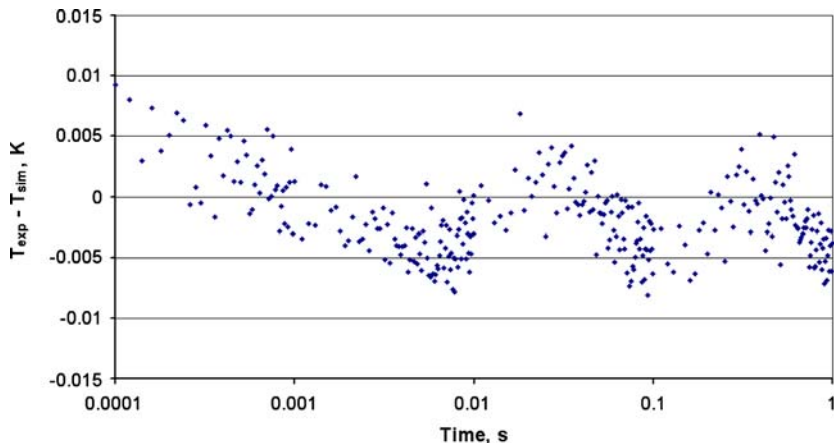


Fig. 5. Deviations between the experimental and simulated temperature rise.

Table I. Physical Properties of the Solders in the Solid State

	Sn60Pb40	Sn62Pb36Ag2	Sn99.3Cu0.7	Sn95.5Ag3.8Cu0.7
Density ($\text{kg} \cdot \text{m}^{-3}$)	8520	8410	7320	7405
Specific heat ($\text{J} \cdot \text{kg}^{-1} \cdot \text{K}^{-1}$)	172	167	220.5	220.7

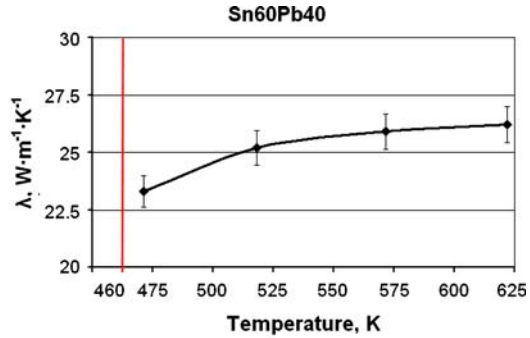
we have been able to reduce this effect and to show that there is a negligible change in the accuracy of the thermal conductivity data.

In order to evaluate the thermal conductivity of the four solders, it has been necessary to identify independently values of the density and heat capacity of the samples. Values of adequate accuracy, which have been published for the solid state [8–10], are listed in Table I; they are used to estimate values for the liquid state. The FE model itself allows the measurement of the product of ρC_P , and the measured values are close to the values for the solid state.

The thermal conductivities for the four samples of solder are given as a function of temperature, and the behavior is shown graphically in Figs. 6 and 7. The experimental results quoted are averages over a number of experiments, and it is estimated that the uncertainty of the final results is approximately $\pm 2\%$ and this is indicated by the bars attached to each point. The vertical line in each plot represents the melting point of the solders.

(a)

Sn60Pb40	
Temperature, K	λ , $\text{W}\cdot\text{m}^{-1}\cdot\text{K}^{-1}$
471.3	23.3
518.2	25.2
571.5	25.9
621.8	26.2



(b)

Sn62Pb36Ag2	
Temperature, K	λ , $\text{W}\cdot\text{m}^{-1}\cdot\text{K}^{-1}$
466.8	22.8
485.3	23.7
518.5	24.9
560.1	26
618.7	26.3

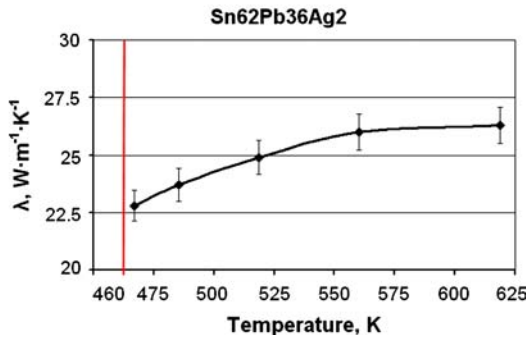


Fig. 6. Thermal conductivity of leaded solders: (a) tin-lead and (b) tin-lead-silver.

The thermal conductivity of both lead-free solders is approximately 25% larger than that for the lead-based solders near their melting points, and this will be significant to the design of appropriate soldering processes in manufacture.

4. CONCLUSIONS

In this paper, we have demonstrated how the thermal conductivity of molten alloys of metals can be determined with an uncertainty of $\pm 3\%$ by means of an appropriate use of the transient hot-wire technique. The work has made use of a more refined finite element model of the experiment than employed previously. We have also reported thermal conductivity data for two lead-free solders designed for electronic production systems for the first time.

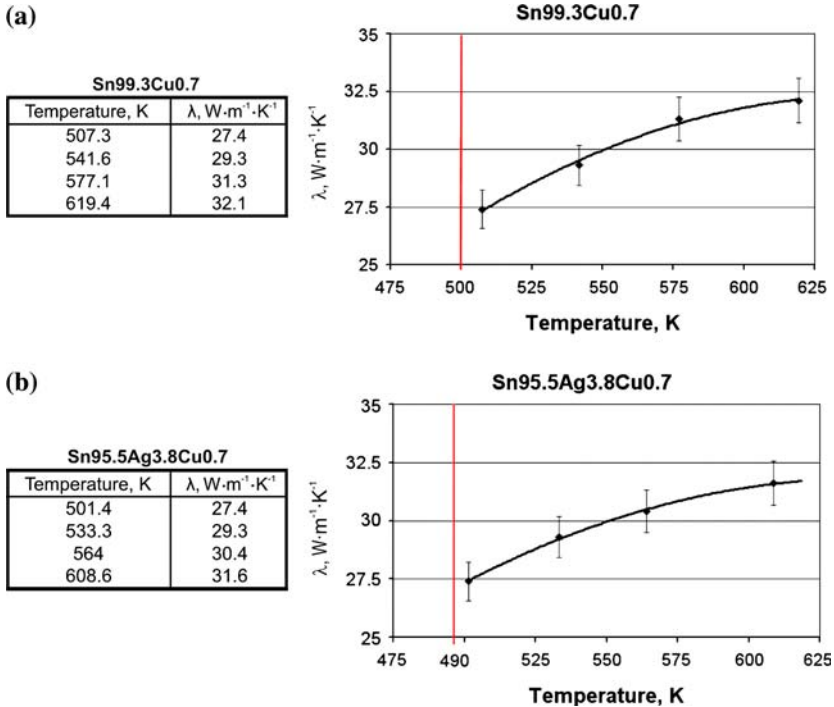


Fig. 7. Thermal conductivity of lead-free solders: (a) tin-copper and (b) tin-silver-copper.

ACKNOWLEDGMENT

The authors would like to acknowledge helpful co-operation with MBO (UK), Ltd., who supplied the solder materials for this project.

REFERENCES

1. European Parliament, Directive 2002/95/EC, European Commission, *Official Journal*, L37 (2003), pp. 19–23.
2. V. M. Peralta-Martinez, *Thermal Conductivity of Molten Metals* (Ph.D. thesis, Imperial College London, 2000).
3. W. A. Wakeham, A. Nagashima, and J. V. Sengers, *Measurement of the Transport Properties of Fluids, Experimental Thermodynamics*, Vol. III (Blackwell Scientific Pubs., Oxford, 1991), pp. 163–172.
4. M. Dix, I. W. Drummond, M. Lesemann, V. M. Peralta-Martinez, W. A. Wakeham, M. J. Assael, L. Karagiannidis, and H. R. van den Berg, "The Thermal Conductivity of Liquid Metals Near Ambient Conditions," *Proc. 5th Asian Thermophys. Props. Conf. (ATPC '98)*, Seoul, Korea (September 1998).

5. R. B. Bird, W. E. Stewart and E. N. Lightfoot, *Transport Phenomena* (Wiley, New York, 1960), pp. 311–317.
6. C. Y. Ho, R. W. Powell, and P. E. Liley, *J. Phys. Chem. Ref. Data* 1:279 (1972).
7. J. Bilek, J. Atkinson, and W. Wakeham, “Validation of FE Model for Transient Hot Wire Thermal Conductivity Measurements,” *Proc. EuroSimE 2005*, IEEE Catalog Number 05EX1050, Berlin, Germany (April 2005).
8. SOLDERTEC Report, *Thermal and Electrical Conductivity of Lead Free Solders*, Lead Free Soldering Technology Centre, <http://www.tintechnology.com/soldertec/soldertec.aspx> (1996).
9. National Physical Laboratory, *Lead Free Properties*, M. Wickham, ed., <http://www.npl.co.uk/ei/iag/leadfree/propertiespbf.html> (2000).
10. Indium Corp. of America, Europe and Asia, *Table of Specialty Alloys and Solders*, <http://www.indium.com/products/alloychart.php> (2002).